

Spatiotemporally periodic solutions by variational methods

Mingtian Liang, Yueheng Lan

School of Physics,

Georgia Institute of Technology, Atlanta 30332-0430, U.S.A.

December 12, 2003

Abstract

The intriguing “Hopf’s last hope”— proposal for a theory of turbulence has significant physical meaning. The problem is how to describe chaotic/turbulent spatiotemporal patterns. Typical system exhibiting spatiotemporal chaos is the Kuramoto-Sivashinsky(KS for short) system. It is a prototype to model the development of turbulence in physical systems. The basic equation is $u_t = (u^2)_x - u_{xx} - \nu u_{xxxx}$. The project mainly studies the chaotic properties of the Kuramoto-Sivashinsky system. The periodic solutions of the system are found by the Newton-Raphson method some other novel variational methods. They are discussed in [2] and [1].

1 Introduction

The standard strategy for solving the Kuramoto-Sivashinsky equation is to expand it in a discrete spatial Fourier series:

$$u(x, t) = \sum_{k=-\infty}^{k=+\infty} b_k(t) e^{ikx}. \quad (1)$$

Since $u(x, t)$ is real,

$$b_k = b_{-k}^*. \quad (2)$$

Substituting (2) into (1) yields the infinite ladder of evolution equations for the Fourier coefficients b_k :

$$\dot{b}_k = (k^2 - \nu k^4)b_k + ik \sum_{m=-\infty}^{+\infty} b_m b_{k-m}. \quad (3)$$

Since

$$\begin{aligned} u_t &= \frac{\partial u(x, t)}{\partial t} \sum_{k=-\infty}^{+\infty} \dot{b}_k(t) e^{ikx}, \\ (u^2)_x &= \left[\left(\sum_{k=-\infty}^{+\infty} b_k(t) e^{ikx} \right) \left(\sum_{k=-\infty}^{+\infty} b_k(t) e^{ikx} \right) \right]_x \\ &= \left(\sum_{k,j} b_k b_j e^{i(k+j)x} \right)_x = \sum_{k,j} (k+j) b_k b_j e^{i(k+j)x} \\ &= \sum_{m=-\infty}^{+\infty} b_m b_{k-m} \quad (\text{let } k = m, j = k - m), \\ -u_{xx} &= \sum_{k=-\infty}^{\infty} k^2 b_k(t) e^{ikx}, \\ -\nu u_{xxxx} &= -\nu \sum_{k=-\infty}^{+\infty} k^4 b_k(t) e^{ikx}, \end{aligned}$$

we get

$$\dot{b}_k = (k^2 - \nu k^4)b_k + ik \sum_{m=-\infty}^{+\infty} b_m b_{k-m}.$$

In the case of b_k are pure imaginary, $b_k = ia_k$, where a_k are real, with the evolution equations

$$\dot{a}_k = (k^2 - \nu k^4)a_k - k \sum_{m=-\infty}^{+\infty} a_m a_{k-m}. \quad (4)$$

This picks out the subspace of odd solutions $u(x, t) = -u(-x, t)$:

From (3) we know that $b_k = b_{-k}^*$, so $ia_k = -ia_{-k}$, $a_k = -a_{-k}$,

$$-u(-x, t) = - \sum_{k=-\infty}^{+\infty} ia_k(t) e^{-ikt} = \sum_{k=-\infty}^{+\infty} ia_{-k}(t) e^{-ikx} = \sum_{k=-\infty}^{+\infty} ia_k(t) e^{ikt} = u(x, t)$$

Thus we have $u(x, t) = -u(-x, t)$.

From (4) we get

$$A_{kj}(a) = \frac{\partial v_k(x)}{\partial a_j} = \frac{\partial}{\partial a_j} ((k^2 - \nu k^4)a_k - k \sum_{m=-\infty}^{+\infty} a_m a_{k-m})$$

The first term remains when $j=k$. For the second term, both $j=m$ or $j=k-m$ terms remain. So

$$A_{kj}(a) = (k^2 - \nu k^4)\delta_{kj} - 2ka_{k-j} \quad (5)$$

When $u(x, t)=0$, the a_{k-j} terms vanishes, so the Jacobian matrix

$$\mathbf{J}^t(0)_{kj} = \delta_{kj} e^{(k^2 - \nu k^4)t}. \quad (6)$$

The trajectories evolve as

$$a(t) = e^{tA}a(0) = \begin{pmatrix} e^{t(k^2 - \nu k^4)} & \dots & 0 \\ & \ddots & \\ 0 & \dots & e^{t(k^2 - \nu k^4)} \end{pmatrix} a(0). \quad (7)$$

When $|k| < 1/\sqrt{\nu}$, $(k^2 - \nu k^4) > 0$. Small perturbations will make the matrix deviate slightly from its eigendirections, but it behaves like the equilibrium one since the diagonal elements still dominate, so $a(t)$ goes up when multiplied by \mathbf{J} . These long wavelength modes of this fixed point are linearly unstable. Similarly, when $|k| > 1/\sqrt{\nu}$, $(k^2 - \nu k^4) < 0$, the elements in \mathbf{J} contract with small perturbations, so the short wave length are stable.

When $\nu > 1$ the $u(x, t)=0$ is the trivial solution, the globally attracting point. All the flame fronts die out quickly. This behavior is observed in the computer calculations. We used the 4th order Rounge-Kuta integration method. When the particular ν goes below 1, bifurcation occurs. The system bifurcates from one steady state to several other steady states. They are studied in detail in [3].

Integrated trajectories of the flow projected onto three or two axes can be drawn. Figure1 shows some typical trajectories projected onto the axes a_1, a_2, a_3 and a_1, a_2, a_6 .

The chaotic behavior of the KS system can be observed with $\nu = 0.029910$. We can study the Poincaré section of the flow [4]. By choosing an arbitrary initial point in the multidimensional space, iterate it with time and calculate its intersection with a certain hyperplane, we can then get the the Poincaré section. The following figure shows a typical Poincaré section of the coefficient a_6 . The Poincaré section is a thin thin line with finite width.

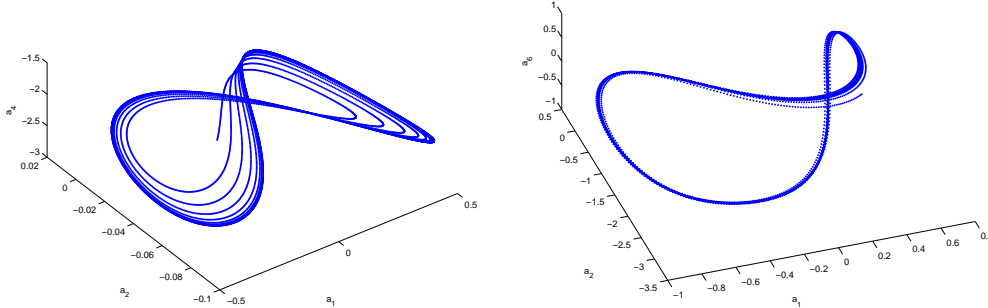


Figure 1: Projections of a typical 16-dimensional trajectory onto three axes. (a) Projections onto the axes a_1, a_2, a_4 . 8000 dots are shown. (b) Projections onto the axes a_1, a_2, a_6 . 6000 dots are shown.

Knowing the method of drawing the Poincaré section, we can now draw the bifurcation tree. The bifurcation tree is drawn on an $a_i - \nu$ plane (Figure(3)). It shows how the location and the periodic properties of the trajectories vary with the parameter ν . First we select an arbitrary initial point in the hyper-plane. Iterate it several times until it settles on the attractor and then we plot one of the coordinates, a_6 to see how it changes in the rest intersections with the Poincaré section. The routine happens all over with different values of ν . The bifurcation tree I have obtained is qualitatively the same as depicted in the Lan's work [4]. The following figure was drawn with the trajectory iterating for about 1200 times for each ν , among them the last 500 points were selected. The initial values for iterating the trajectories are:

The bifurcation points are different with different initial values. I got

a_1	a_2	a_3	a_4	a_5	a_6	a_7	a_8
-0.0000	-0.1197	-0.0381	-0.4586	-1.4400	-1.4400	-0.2644	-0.1603
a_9	a_{10}	a_{11}	a_{12}	a_{13}	a_{14}	a_{15}	a_{16}
-0.8729	-0.2379	-0.6458	-0.9669	-0.6649	-0.8704	-0.0099	-0.1370

a period-4 window at $\nu = 0.029972$. This may also be the cause of the deviation in the above $a_6(n+1) - a_6(n)$ Poincaré section. The following figure demonstrates the different results of the different initial values.

For the strange attractor at $\nu = 0.029910$, the system is chaotic—highly sensitive to small uncertainties in the specification of the initial state. This is observed with the trajectory pictures generated by Runge-Kuta integration method. We evaluate it quantitatively by finding the Lyapunov exponent. As we assume that the displacement of the trajectories may increase expo-

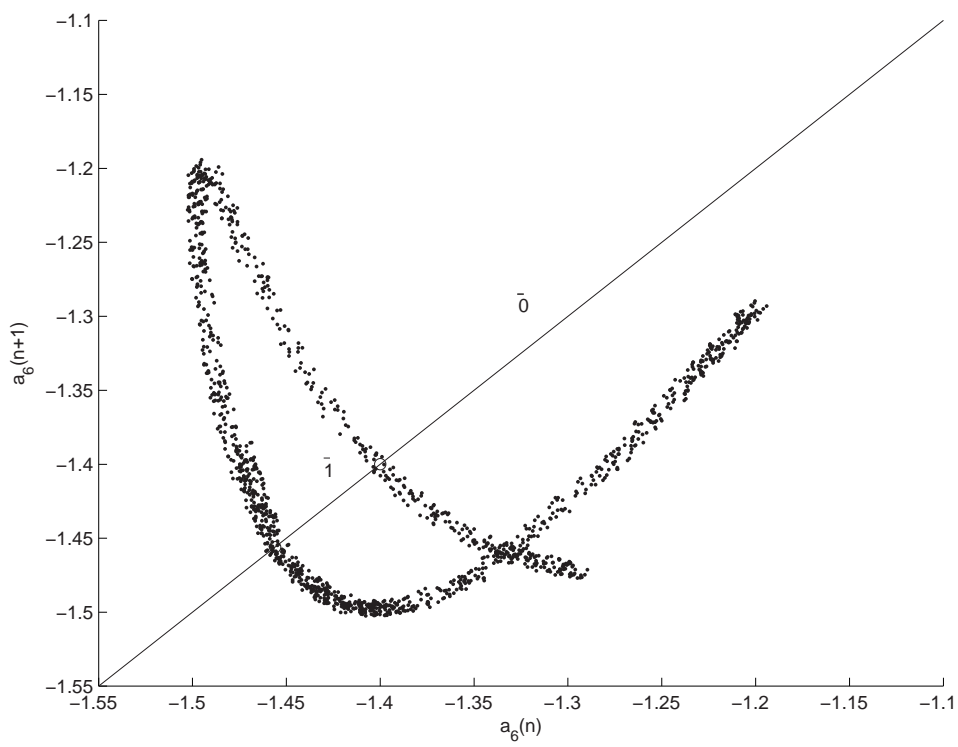


Figure 2: The Poincaré section of Figure 1 with $a_1=0$. The $\bar{0}, \bar{1}$ points shown are the 1-cycle periodic orbits.

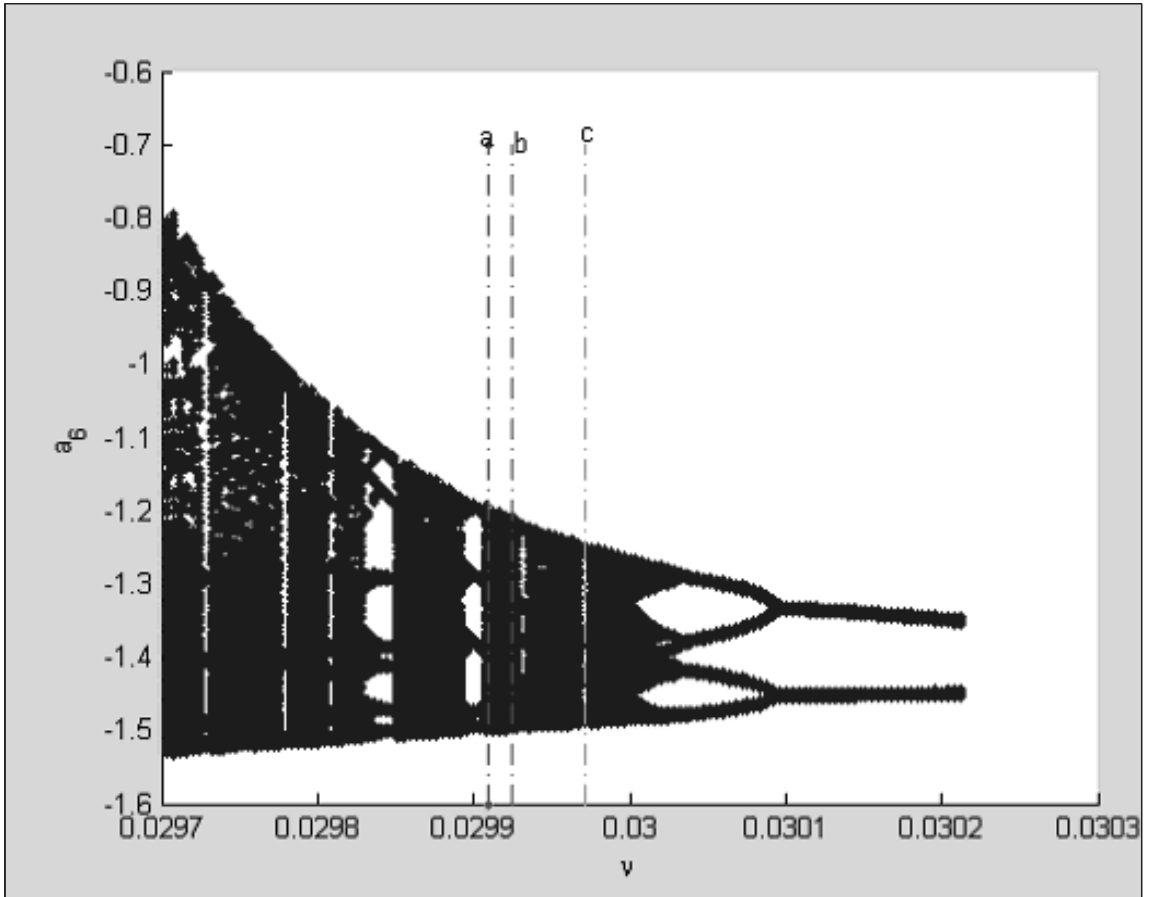


Figure 3: Period doubling tree for coordinate a_6 Truncation $N=16$ of the Fourier modes. Line a and line b indicate the result of the work in [1], with the values $\nu = 0.029910$ (chaotic) and $\nu = 0.029924$ (period-3 window). I found a period-4 window is at $\nu = 0.029972$, indicated by line c on the right.

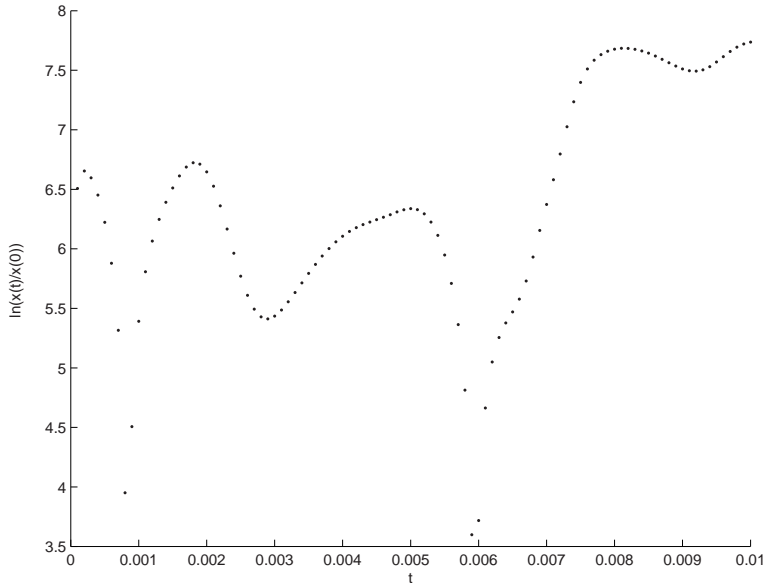


Figure 4: A numerical approach to find the Lyapunov exponents.

nentially, the Lyapunov exponent can be defined as λ in the equation

$$|\delta x(t)| \approx e^{\lambda t} |\delta x(0)| \quad (8)$$

where $\delta x(0)$ and $\delta x(t)$ are the initial and final displacements of the trajectories. The Lyapunov exponent is then calculated by

$$\lambda = \lim_{t \rightarrow \infty} \left\{ \frac{1}{t} \ln \frac{\delta x(t)}{\delta x(0)} \right\} \quad (9)$$

In search of the Lyapunov exponent we can do it by solving the the KS equations. Since by definition the Jacobian matrix is

$$\lim_{\delta x \rightarrow 0} \frac{\delta x_i(t)}{\delta x_j(0)} = \frac{\partial x_i(t)}{\partial x_j(0)} = \mathbf{J}_{ij}^t(x_0), \quad (10)$$

so the leading Lyapunov exponent can be computed from the linear approximation. The Lyapunov exponents are the eigenvalues of the Jacobian matrix. The numerical tests can be implemented by iterating the trajectories. If we get the stable solutions, we can iterate it conversely. Figure(4) shows a result with arbitrary initial state. There are several folds and the segments have different slopes corresponding to different Lyapunov exponents.

We use the Newton-Raphson method to find the cycles. The method is based on the linear approximation of function $F(x) = x - f(x)$ around its

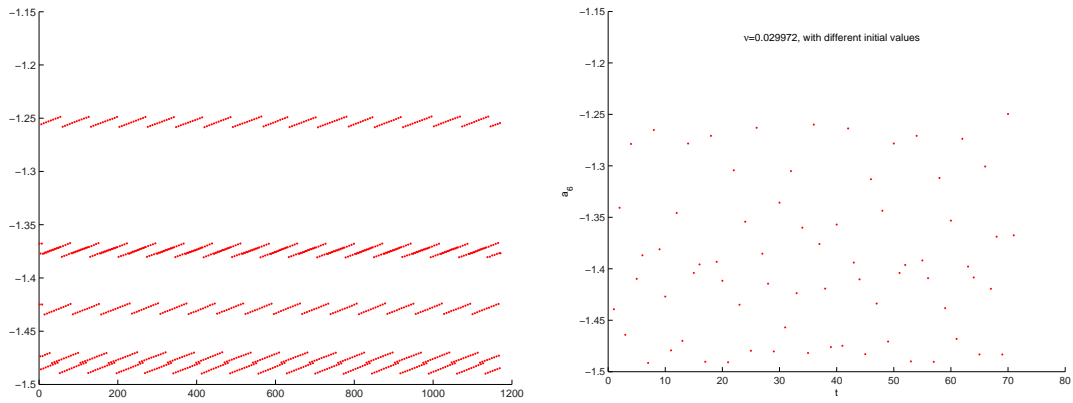


Figure 5: The Poincaré section of Figure 1 drawn by a_6 versus time. When the initial values vary, the near periodic cycle (left) becomes chaotic (right).

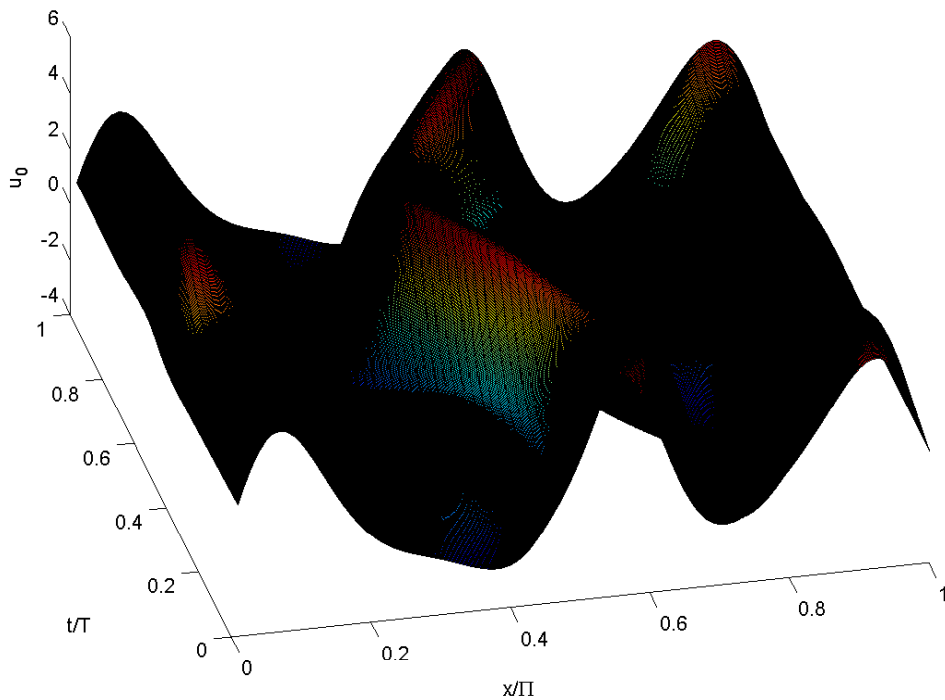


Figure 6: Spatiotemporally periodic odd solution $u_0(x, t)$. $N=16$ Fourier modes were truncated with $\nu = 0.029910$. The x axis is divided by period π while the t axis is divided by the period T

starting guess x_0 :

$$F(x) \approx F(x_0) + F'(x_0)(x - x_0) \quad (11)$$

An approximate solution x_1 of $F(x)=0$ is

$$x_1 = x_0 - F(x_0)/F'(x_0) \quad (12)$$

For a system with n steps and d dimensions, the equations become $nd \times nd$. To do this, we can do a "grid search" of the system. That is, we divide the flow into n steps in time and m points in space.

Rather than Newton-Raphson method, a new "Newton Descent" method is introduced in [2]. With a fictitious time parameter, the time steps are varied to avoid the overshooting of the zeros we are trying to get.

From the poincaré section of a_6 , we can also see the one-dimensional approximation is reasonable for getting the cycles and from this method we can compute the Lyapunov exponents also. In this poincaré figure, there are three branches. We can use the least square rule to fit these branches with polynomial functions $f_1(x)$, $f_2(x)$, $f_3(x)$. Then finding the cycles remain the routine calculation of the Newton-Raphson method.

After a few trials of random initial values, I didn't get any chaos for $N < 9$. The trajectories diverge rapidly or converge to the trivial solution $u(x, t)=0$.

The odd solutions of $u_0(x, t)$, were derived from the Fourier coefficients. We now go back to construct the original $u_0(x, t)$. Figure(6) is one of the typical chaotic attractors in the symmetry unrestricted space.

2 Discussion

There are open questions for this KS system problem, e.g. what is the behavior of the KS system with larger ν or in the whole complex plane? How can we find cycles more efficiently? How to improve the robustness of the Newton's method? What other methods can we use other than grid search method? By introducing and implementing the efficient methods, we can get full understanding of the KS system and can use such experience to study other systems with significant physical importance.

References

- [1] Cvitanović and Lan, *Turbulent fields and their recurrences*, Workshop on Multiparticle Production: Correlations and Fluctuations in QCD (World Scientific, Singapore 2003).
- [2] Lan and Cvitanovic, *Variational method for finding periodic orbits in a general flow*, Phys. Rev. **E** 2003
- [3] G.Kevrekidis; Nicolaenko; C. Scovel, *Back in the saddle Again: A computer Assisted Study of the Kuramoto-Sivashinsky Equation*, SIAM Journal on Applied Mathematics, **50** (1990) 760-690
- [4] F.Christiansen, P.Cvitanović and V. Putkaradze *Spatiotemporal Chaos in Terms of Unstable Recurrent Patterns*, Nonlinearity **10** (1997) 55-70